Universal Temperature Model for Shallow Algal Ponds Provides Improved Accuracy

ARTICLE *in* ENVIRONMENTAL SCIENCE & TECHNOLOGY · MARCH 2011

Impact Factor: 5.33 · DOI: 10.1021/es1040706 · Source: PubMed

5 AUTHORS, INCLUDING:

Quentin Béchet
Massey University
10 PUBLICATIONS **142** CITATIONS
SEE PROFILE

Jason Park
National Institute of Water and Atmospheric …
22 PUBLICATIONS **698** CITATIONS
SEE PROFILE

Benoit Guieysse
Massey University
75 PUBLICATIONS **2,720** CITATIONS
SEE PROFILE

Environmental Science & Technology

ARTICLE

pubs.acs.org/est

Universal Temperature Model for Shallow Algal Ponds Provides Improved Accuracy

Quentin Béchet,[†] Andy Shilton,[†] Jason B. K. Park,[‡] Rupert J. Craggs,[‡] and Benoit Guieysse*[,†]

[†]Center for Environmental Technology and Engineering, School of Engineering and Advanced Technology, Massey University, Private Bag 11 222, Palmerston North 4442, New Zealand

[‡]National Institute of Water and Atmospheric Research (NIWA), P.O. Box 11-115, Hamilton, New Zealand

Supporting Information

ABSTRACT: While temperature is fundamental to the design and optimal operation of shallow algal ponds, there is currently no temperature model universally applicable to these systems. This paper presents a model valid for any opaque water body of uniform temperature profile. This new universal model was tested against 1 year of experimental data collected from a wastewater treatment high rate algal pond. On the basis of 1 year of data collected every 15 min, the average errors of the predicted afternoon peak and predawn minimum were both only 1.3 °C and the average error between these extremes was just 1.2 °C. In order to demonstrate the improvement in accuracy gained, the expressions for heat fluxes used in nine prior temperature models were systematically substituted into the new universal model and evaluated against the experimental data. Errors in the peak and minimum temperatures increased by up to 2.1 and 3.2 °C, respectively, while the error between these extremes increased by up to 2.9 °C. In practical applications, these levels of inaccuracies could lead to an under/overestimation of the algal productivity and the evaporative water loss by approximately 40% and 300%, respectively.

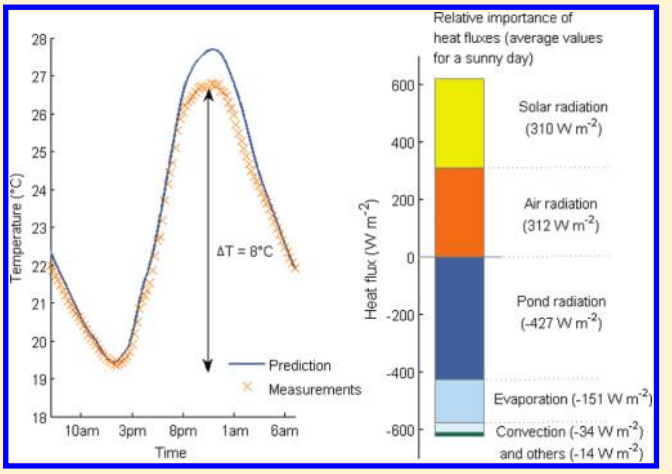

INTRODUCTION

Evaluating the economical feasibility and sustainability of processes incorporating shallow algal ponds requires the ability to forecast the productivity of these systems and their environmental impact. For this purpose, it is necessary to accurately predict the pond water temperature.

In the first instance, accurately predicting the pond temperature is important because temperature influences the rate of various reactions of photosynthesis.[1] This temperature dependence causes

(i) algae to exhibit optimal growth only within a narrow temperature range,
(ii) algae to die above a certain temperature threshold, and
(iii) algal light-saturation to occur at relatively low light intensity at low temperature, for example, in the morning.

Second, an accurate temperature model can also be used to optimize temperature control strategies to maximize algal productivity by estimating the amount of heat to add to or remove from the pond. Examples of temperature control strategies in the literature include

(i) maintaining optimum temperature at all times,[2]
(ii) reducing temperature to prevent growth inhibition at high temperatures,[3] and
(iii) raising temperature in the morning to optimize light utilization efficiency.[4]

Finally, accurate temperature prediction is important because evaporation from shallow algal ponds is positively correlated with the water temperature.[5] This means that the temperature directly affects the green and blue water footprint of these processes, typically defined as the volume of evaporative water loss per unit of biomass produced.[6]

Various models for predicting water temperature in lakes, wastewater treatment ponds, aquaculture ponds, and other similar systems have been described in the literature (e.g., refs 7−10). However, these prior models cannot be universally applied because the expressions of certain heat fluxes, the evaporative heat flux in particular, are derived from empirical relationships specific to the type of system studied.[7−10]

The objective of this paper is to present the first universal model for temperature prediction in shallow algal ponds validated against data obtained from over 1 year of experimental

Received: December 5, 2010
Accepted: March 8, 2011
Revised: March 1, 2011
Published: March 29, 2011

monitoring of a high rate algal pond. This model is based on eight heat fluxes that use input parameters from readily available field data (meteorological data, site characteristics) and is valid for any opaque water body of a uniform temperature profile. The accuracy of the new universal model is compared to that of prior models published in the literature. The modeling includes a thorough sensitivity analysis conducted to determine the uncertainty generated by various input parameters. Finally, predictions of algal productivity and evaporative water loss using the new universal temperature model are demonstrated to be more accurate than those from using other temperature models.

MATERIALS AND METHODS

The temperature data used to validate the model was collected from a pilot-scale wastewater treatment high rate algal pond at National Institute of Water and Atmospheric Research's (NIWA) Ruakura Research Centre, Hamilton, New Zealand (37°47′S, 175°19′E). The pond had the following dimensions: volume, 8.1 m^3; surface area, 31.8 m^2; and depth, 0.3 m. A paddlewheel ensured complete mixing. The pond was operated on a fed-batch regime with an average hydraulic retention time of 4−8 days, depending on the season. Water was added every hour (for example, 55 L of water per hour was added to the pond for a hydraulic retention time of 6 days). The concentration of suspended solids was on the order of 0.3 g L^{-1} and algae productivity was between 9.0 and 17 g m^{-2} d^{-1}. The soil beneath the pond was a wet clay. The algae raceway pond used for model validation was fed with domestic wastewater, but the influence of the heat released by heterotrophic bacteria during growth was neglected. A more detailed description of the pond, its wastewater treatment performance, and algal productivity can be found in ref 11.

Meteorological data used in the model were taken from a weather station located less than 1 km away from the pond (C75734 Hamilton Ruakura 2EWS Climate Station[12]). Solar irradiance, air temperature, wind velocity, relative humidity, and rainfall were collected hourly and cloud cover daily. Pond temperature was collected and logged at 15 min intervals.

Modeling Approach. The pond was assumed completely mixed and all physical properties were assumed to be that of water under standard conditions. Every radiating body was considered as a gray-diffuse surface. The pond was assumed to be deep enough to absorb all radiative fluxes from the environment. In other words, air and solar radiation were assumed to be fully absorbed by the water before reaching the pond base. This assumption was based on the fact that light only penetrates two-thirds of the actual culture depth under typical algae cultivation field operation.[13] The fraction of solar radiation converted by algae into algal biomass during photosynthesis was assumed to be constant and equal to 2.5%.[14] The model inputs (solar irradiance, air temperature, wind velocity, relative humidity, rainfall, and inflow temperature) are described below with other specific assumptions.

Description of the Model. A heat balance analysis for the pond water can be described as

$$\rho_w V C_{p_w} \frac{dT_p}{dt} = Q_{ra,p} + Q_{ra,s} + Q_{ra,a} + Q_{ev} + Q_{conv} + Q_{cond} + Q_i + Q_r \quad (1)$$

where T_p is the pond temperature (K); ρ_w and C_{p_w} are the density (kg m^{-3}) and the specific heat capacity (J kg^{-1} K^{-1}) of pond water, respectively; V is the pond volume (m^3); $Q_{ra,p}$ is the radiation from the pond surface (W); $Q_{ra,s}$ is the total (direct + diffuse) solar radiation (W); $Q_{ra,a}$ is the radiation from the air to the pond (W); Q_{ev} is the evaporation flux (W); Q_{conv} is the convective flux at the pond surface (W); Q_{cond} is the conductive flux with the ground at the pond bottom (W); Q_i is the heat flux associated with the water inflow (W); and Q_r is the heat flux induced by rain (W) (Supporting Information, S1).

Pond Radiation. Because the water surface is assumed to be gray-diffuse, radiation from the pond surface to the atmosphere is given by Stefan−Boltzmann's fourth power law[15]

$$Q_{ra,p} = -\varepsilon_w \sigma T_p^4 S \quad (2)$$

where ε_w is the emissivity of water (0.97 is used, which is typical for water[9]), σ is the Stefan−Boltzmann constant (W m^{-2} K^{-4}), and S is the pond surface area (m^2).

Solar Radiation. The heat flux received by the pond from solar radiation can be calculated on the basis of the total (direct + diffuse) solar irradiance at ground level, H_s (W m^{-2}):[15]

$$Q_{ra,s} = (1 - f_a) H_s S \quad (3)$$

where f_a is the photosynthetic efficiency (the fraction of sunlight converted by algae into chemical energy during photosynthesis). When the pond is in the shade of external elements, such as trees or buildings, eq 3 can be adjusted by adding a "shadow function" (see ref 16). The component of solar radiation that is reflected was assumed to be negligible (Supporting Information, S2).

Air Radiation. According to the Stefan−Boltzmann's fourth power law, the radiative flux $Q_{ra,a}$ (in W m^{-2}) generated by air at a temperature of T_a (K) is given by[15]

$$Q_{ra,a} = \varepsilon_w \varepsilon_a \sigma T_a^4 S \quad (4)$$

where ε_a is the emissivity of the air (also called the atmospheric coefficient). Determination of the air emissivity is given in the Supporting Information (S3). Water reflectivity was not taken into account in this expression for the same reasons it was neglected in the expression of solar radiation heat flux.

Evaporation. The rate of evaporation m_e (kg s^{-1} m^{-2}) is related to the evaporative heat flux Q_{ev} by

$$Q_{evap} = -m_e L_w S \quad (5)$$

where L_w is the water latent heat (J kg^{-1}). The rate of evaporation from a water surface has been the object of numerous studies in the past.[17] However, the formulas expressing the rate of evaporation have been derived from experimental studies and most of them are too specific to the system studied to be applicable to a general model that will be suitable for ponds operated in different locations and climates.[17] In an alternative theoretical approach based on the application of the Buckingham theorem,[5] the evaporation rate can be shown to depend on three dimensionless numbers

$$\text{the Sherwood number}: \quad Sh = \frac{KL}{D_{w,a}} \quad (6a)$$

$$\text{the Schmidt number}: \quad Sch = \frac{\nu_a}{D_{w,a}} \quad (6b)$$

$$\text{the Reynolds number}: \quad Re_L = \frac{Lv}{\nu_a} \quad (6c)$$

dx.doi.org/10.1021/es1040706 |Environ. Sci. Technol. 2011, 45, 3702–3709

where K is the mass transfer coefficient (m s^{-1}), L is the characteristic pond length (m), $D_{w,a}$ is the mass diffusion coefficient of water vapor in air (m^2 s^{-1}), ν_a is the air kinematic viscosity (m^2 s^{-1}), and v is the wind velocity (m s^{-1}) at a given elevation from the pond surface. The Buckingham theorem links these three parameters as follows:

$$Sh_L = A(Re_L)^{\beta}(Sch)^{\delta} \quad (7)$$

where A, β, and δ are dimensionless coefficients that depend on the surface shape (e.g., cylindrical, horizontal, etc.) and on the nature of the flow (laminar or turbulent). For a horizontal surface, eq 7 becomes:[5]

$$Sh_L = 0.035(\mathrm{Re}_L)^{0.8}(Sch_L)^{1/3} \quad \text{for } Re_L > 5 \times 10^5 \text{ (turbulent flow)} \quad (8a)$$

$$Sh_L = 0.628(Re_L)^{0.5}(Sch_L)^{1/3} \quad \text{for } Re_L < 3 \times 10^5 \text{ (laminar flow)} \quad (8b)$$

The mass transfer coefficient K can be determined using eqs 8a and 8b, and the evaporation rate m_e is given by

$$m_e = K\left(\frac{P_w}{T_p} - \frac{\mathrm{RH} \times P_a}{T_a}\right)\frac{M_w}{R} \quad (9)$$

where T_a is the air temperature (K), P_a and P_w are the saturated vapor pressure (Pa) at T_a and T_p, RH is the relative humidity of the air over the pond surface, M_w is the molecular weight of water (kg mol^{-1}), and R the ideal gas constant (Pa m^3 mol^{-1} K^{-1}). P_a and P_w can be determined using[18]

$$P_i = 3385.5 \exp[-8.0929 + 0.97608(T_i + 42.607 - 273.15)^{0.5}] \quad (10)$$

There is no clear consensus in the literature on which elevation is most appropriate for quantifying the wind velocity used in the above application.[17] Eqs 8a and 8b were derived for situations when the wind is constant with respect to height prior to reaching the edge of a horizontal boundary. Thus, in this theoretical situation the value of wind velocity used in the Reynolds number (eq 6c) is assumed to be equal to this constant value. However, in the real world situation of an outdoor pond, the wind velocity varies with the height above the pond surface. Thus, in practical application the height at which the wind velocity was determined was equal to the boundary layer thickness where the wind velocity is not retarded by surface drag. The height δ_L at which the wind velocity was determined can be calculated as:[19]

$$\delta_L = L(0.381{Re_L}^{-1/5} - 10256{Re_L}^{-1}) \quad (11)$$

In the case of the pond used for validation in the present study, the boundary layer height was estimated to be around half a meter above the pond surface, a value well within the 0.3−2.0 m range proposed by ref 17. Interestingly, when the wind velocity was determined at this elevation, eq 9 predicted almost exactly the same amount of evaporation as the experimental formula derived to predict evaporation from small lakes,[8] which gave further confidence to this approach.

If wind data is not available at the boundary layer height, a power law can be used to determine the wind velocity v at a height z knowing the wind velocity v_0 at a height z_0

$$v(z) = v_0\left(\frac{z}{z_0}\right)^{\alpha} \quad (12)$$

where α is the power law exponent and is a function of obstructions surrounding the pond (e.g., trees, buildings, etc.[20]).

Convection. As heat transfer and mass transfer obey to the same laws, the convective heat flux Q_{conv} can be expressed in a similar manner to the evaporative heat flux. Application of the Buckingham theorem to convection at the pond surface thus yields three dimensionless numbers:[5]

the Nusselt number :

$$Nu_L = \frac{h_{conv}L}{\lambda_a} \quad \text{(analogous to the Sherwood number)} \quad (13a)$$

the Prandtl number :

$$Pr = \frac{\nu_a}{\alpha_a} \quad \text{(analogous to the Schmidt number)} \quad (13b)$$

the Reynolds number : $$Re_L = \frac{Lv}{\nu_a} \quad (13c)$$

where h_{conv} is the convection coefficient (W m^{-2} K^{-1}), λ_a is the air thermal conductivity (W m^{-1} K^{-1}), and α_a is the air thermal diffusivity (m^2 s^{-1}). As convection and evaporation obey to the same law, the relationship between these three numbers uses the same coefficients A, β, and δ:

$$Nu_L = 0.035(Re_L)^{0.8}(Pr)^{1/3} \quad \text{for } Re_L > 5 \times 10^5 \text{ (turbulent flow)} \quad (14a)$$

$$Nu_L = 0.628(Re_L)^{0.5}(Pr)^{1/3} \quad \text{for } Re_L < 3 \times 10^5 \text{ (laminar flow)} \quad (14b)$$

The convective flux Q_{conv} is given by

$$Q_{conv} = h_{conv}(T_a - T_p)S \quad (15)$$

Conduction. An expression of the conductive heat flux between the pond bottom and the soil beneath it originates from Fourier's law

$$Q_{cond} = k_s S\frac{dT_s}{dz}(z = 0) \quad (16)$$

where k_s is the soil thermal conductivity (W m^{-1} K^{-1}), T_s is the soil temperature (K), and z is the depth (m). To determine the gradient of temperature in the soil under the pond, the soil temperature profile has to be determined by solving the heat equation in the soil beneath the pond, assuming the soil temperature T_s is a function of the depth z and the time t:

$$C_{p_s}\rho_s\frac{dT_s}{dt}(z,t) = k_s\frac{d^2T_s}{dz^2}(z,t) \quad (17)$$

where C_{p_s} is the soil specific heat capacity (J K^{-1} kg^{-1}) and ρ_s is the soil density (kg m^{-3}). The thermal characteristics of several types of soil are found in ref 21.

Table 1. Constants and Parameter Values for the Pond in New Zealand and Input Variables[a]

symbol	definition	unit	value
	Water Constants		
ρ_w	water density	kg m^{-3}	998
C_{p_w}	water heat capacity	J kg^{-1} K^{-1}	4.18 × 10^3
L_w	water latent heat	J kg^{-1}	2.45 × 10^6
ε_w	water emissivity	–	0.97
M_w	water molecular weight	kg mol^{-1}	0.018
	Soil Constants		
k_s	**soil thermal conductivity**	**W m^{-1} K^{-1}**	**1.7**
C_{p_s}	**soil specific heat capacity**	**J kg^{-1} K^{-1}**	**1.25 × 10^3**
ρ_s	**soil density**	**kg m^{-3}**	**1.9 × 10^3**
$T_{s,ref}$	soil temperature at $l_{s,ref}$	°C	13.6
	Air Constants		
ε_a	**air emissivity**	–	**0.8**
ν_a	air kinematics viscosity	m^2 s^{-1}	1.5 × 10^{-5}
λ_a	air thermal conductivity	W m^{-1} K^{-1}	2.6 × 10^{-2}
Pr_a	air Prandtl number	–	0.7
ρ_a	air density	kg m^{-3}	1.2
α_a	air thermal diffusivity	m^2 s^{-1}	2.2 × 10^{-5}
$D_{w,a}$	mass diffusion coefficient of water vapor in air	m^2 s^{-1}	2.4 × 10^{-5}
	Pond constants		
V	pond volume	m^3	8.1
S	pond surface	m^2	31.8
z	**wind velocity height**	**m**	**0.5**
z_0	wind sensor height	m	10
q_i	inflow rate	m^3 s^{-1}	1.5 × 10^{-5}
f_a	**algal absorption fraction**	%	**2.5**
L	pond characteristic length	m	10
α	**power law exponent**	-	**0.29**
φ	site latitude	deg	−37.9°
	Universal Constants		
σ	Stephan−Boltzmann constant	W m^{-2} K^{-4}	5.67 × 10^{-8}
R	ideal gas constant	Pa m^3 mol^{-1} K^{-1}	8.314
	Input Variables		
T_a	**air temperature**	**°C**	
H_s	**solar irradiance**	**W m^{-2}**	
RH	**relative humidity**	–	
v	**wind velocity**	**m s^{-1}**	
q_r	**rain waterflow**	**m^3 m^{-2} s^{-1}**	

[a] The most uncertain parameters are written in bold characters and were tested in a sensitivity analysis (Figure 3).

The first boundary condition is given by the fact that the temperature at the surface of the soil (at $z = 0$) is equal to the water temperature in the pond (see Supporting Information, S4). The second boundary condition is given by the value of the soil temperature $T_{s,ref}$ at the depth $l_{s,ref}$, where $l_{s,ref}$ is the depth at which the soil temperature is constant over the year. $T_{s,ref}$ is generally assumed to equal the annual average temperature and $l_{s,ref}$ can be estimated with the eq 18[5]:

$$l_{s,\,ref} = 4400(\alpha_s)^{1/2} \tag{18}$$

where α_s is the soil thermal diffusivity (m^2 s^{-1}). Initially, the temperature profile is assumed to be linear, which yields the following set of initial and boundary conditions (Supporting Information, S4):

$$T_s(t, z = 0) = T_p(t) \tag{19a}$$

$$T_s(t, z = l_{s,\,ref}) = T_{s,\,ref} \tag{19b}$$

$$\frac{d^2 T_s}{dz^2}(t = 0) = 0 \tag{19c}$$

Solving the heat equation (eq 17) yields the soil temperature profile $T_s(z,t)$ and therefore the value of the soil temperature gradient under the pond (at $z = 0$).

dx.doi.org/10.1021/es1040706 |Environ. Sci. Technol. 2011, 45, 3702–3709

Inflow Heat flux. The heat flux associated with the water inflow (q_i, $m^3\ s^{-1}$) can be expressed as

$$Q_i = \rho_w C p_w q_i (T_i - T_p) \quad (20)$$

assuming that the water inflow is at temperature T_i and that the outflow is at temperature T_p.

Rain Heat Flux. Rainwater is assumed to be at air temperature. The heat flux Q_r from the rainwater flow (q_r, $m^3\ m^{-2}\ s^{-1}$) can be expressed as

$$Q_r = \rho_w C p_w q_r (T_a - T_p) S \quad (21)$$

Computations and Methods for Results Analysis. The equations described in the model section were computationally integrated in time using MATLAB software (The MathWorks, Natick, MA). A first-order forward Euler algorithm was used with a 1 s time step. A first-order Euler scheme in time and a second-order scheme in space (with a 1 cm length step) were used to solve the heat equation in the soil (eq 17). As an initial value, the pond temperature was set at the experimental temperature measured at midnight at the first day of simulation. Meteorological data were interpolated linearly between the data points. Experimental data were available over nearly an entire year (February 1, 2008 to January 30, 2009). A total of 20 days were excluded from the data set because no pond temperature data was collected (e.g., pond temperature value was 0 for several days, etc.). The details on the data set selection are given in the Supporting Information (S5). The inflow temperature was taken equal to the soil temperature $T_{s,ref}$.

Three criteria were used to define the accuracy of the model: (i) the average error in the estimation of the afternoon peak temperature (absolute value, over the 345 days considered), (ii) the average error in the estimation of the predawn minimum temperature (absolute value, over the 345 days considered), and (iii) the average error in the estimation of the temperature prediction between the afternoon peak and predawn minimum (absolute value, over the 345 days considered) (Supporting Information, S6).

To assess the accuracy of the new universal model compared to nine prior models published in the literature, the alternative expressions of heat fluxes used in the prior models were systematically substituted into the new universal model and evaluated against the experimental data. Because the expressions of pond radiation, air radiation, and the heat flux associated with the water inflow were identical in all the prior models (Supporting Information, S7), this evaluation was limited to considering

(i) one expression for the solar radiation based on a theoretically based calculation of solar irradiance,
(ii) four expressions of the evaporative and convective heat fluxes (these fluxes were considered together because they rely on the same fundamental laws), and
(iii) a simple expression of the conductive flux.

Furthermore, the effect of neglecting the conductive and rainwater fluxes on temperature prediction accuracy was evaluated. A detailed rationale and description of the heat flux expressions selected for comparison can be found in the Supporting Information (S8).

Finally, because various input parameters cannot be determined with a high level of accuracy, a sensitivity analysis was undertaken to quantify their impact on the temperature prediction. The input parameters which were identified as requiring investigation were

(1) the air emissivity, ε_a, which is a function of several meteorological parameters (air temperature, relative humidity, different atmospheric gas concentrations, etc) and thus cannot be tightly defined;[22]
(2) the soil thermal characteristics (k_s and α_s), which are only defined for specific types of soil and there can be a wide range of thermal behaviors between different soil types;[21]
(3) the power law exponent (α), which is a function of the environment (trees, buildings, etc.) and so is a subjective coefficient;[20]
(4) the height z at which the wind velocity must be measured; as discussed in the modeling section, z is not clearly defined in the literature and has a range between 0.3 and 2 m;[17] and
(5) the photosynthetic efficiency (f_a), which varies depending on the cultivation conditions such as light intensity, temperature, etc.

The upper and lower extremes of all the above input parameters were tested in the new universal model, and their influence on the temperature prediction accuracy was quantified. Uncertainty from weather data was also evaluated by varying the solar irradiance, wind velocity, and relative humidity by ±10% and the air temperature by ±1 °C. Table 1 lists the parameters used in the new universal model.

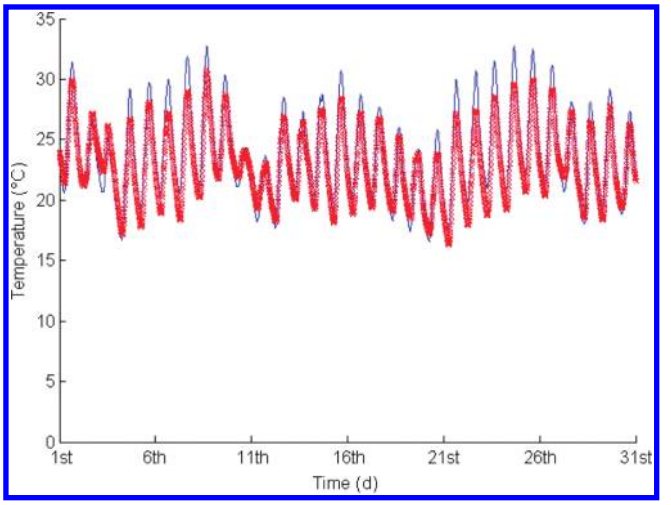

Figure 1. Predicted (blue line) and measured (red crosses) temperature profiles in the high rate algal pond over the month of January 2009.

RESULTS AND DISCUSSION

Model Accuracy. The ability of the new universal model to predict the temperature of the high rate algal pond was determined on the basis of 33 221 data points representing a year of operation. Figure 1 illustrates the excellent fit between the experimental and predicted temperature profiles for the month of January 2009 with all other months shown in the Supporting Information (S5). The average errors in the estimation of the afternoon peak and predawn minimum temperatures were both 1.3 °C, and the average error in the temperature difference between the afternoon peak and predawn minimum was 1.2 °C. The model had a tendency to slightly overestimate daily peak temperature and underestimate temperature during the winter

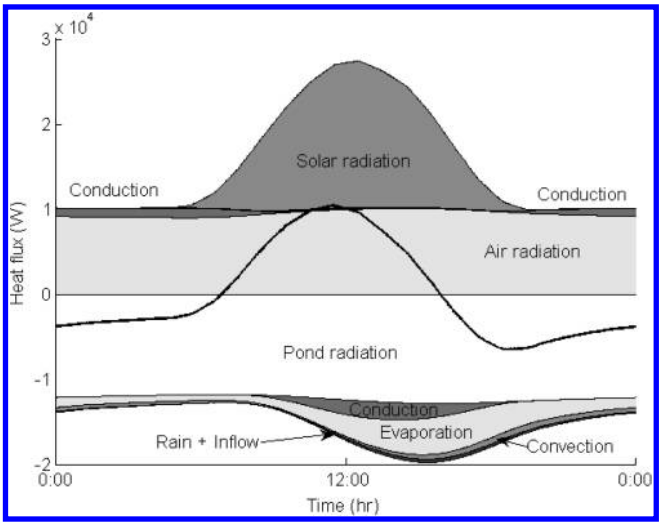

Figure 2. Changes in heat fluxes (annual average) reaching the high rate algal pond. The thick plain line represents the total heat flux. The value of each heat flux at time t was computed as the average of the heat flux over the year at this time.

months (Supporting Information, S5). Two possible explanations for these trends are (1) that air emissivity was assumed to be constant through time, although it is actually a function of meteorological parameters,[22] and (2) the impact of the paddle wheel on shading and evaporation in the pilot-scale pond used for validation was neglected (see Supporting Information, S5, for further explanations). While it is possible to improve the fit of the prediction for the pond located in New Zealand by adjusting key input parameters, this was not attempted because this study aimed to develop a universal model for temperature prediction rather a model optimized for a specific location.

Figure 2 shows that, on a yearly basis, the air radiation and pond radiation generally compensate each other. The pond radiation is proportional to the pond temperature to the fourth, while the air radiation is proportional to the air temperature to the fourth (eqs 2 and 4). As the pond and air temperatures generally differed by less than 10 °C, their values in kelvin are relatively similar, and the two heat fluxes tend to balance themselves. Therefore, solar radiation was mainly responsible for temperature raise at daytime, whereas conduction and evaporation were the main contributors to cooling at dusk. These different contributions may explain why the model was slightly less accurate during winter (Supporting Information, S5) because there is less uncertainty on the prediction of the solar heat flux than other heat fluxes.

Comparison with Other Temperature Models. In order to assess the relative accuracy of the new universal model, alternative heat flux expressions used in nine prior models were systematically substituted into the new universal model and evaluated against the experimental data. Full details are found in the Supporting Information (S8). The average errors in the estimations of the new universal model are compared against the average errors in the estimations of the prior models in Table 2. The errors in the estimated temperatures for the afternoon peak and predawn minimum increased from 1.3 to 2.1 and 3.2 °C respectively, while the error in the temperature difference between the afternoon peak and predawn minimum increased from 1.2 to 2.9 °C.

As previously discussed, the expressions for pond radiation, air radiation, and the heat flux associated with the inflow used in the new universal model have been used in prior models. With regard to the other five heat fluxes our analysis showed the following.

(1) Solar radiation represented 35% of the heat gain in average over the year (Figure 2) and therefore made a high contribution to the overall accuracy. A net improvement in accuracy was therefore obtained by using on-site irradiance data as opposed to an estimate based on cloud cover data (Table 2).
(2) The evaporative heat flux represented up to 22% of the total heat loss (Figure 2). Consequently, modeling convection and evaporation using expressions empirically derived from different systems (e.g., mechanically agitated ponds) significantly reduced accuracy (Table 2).
(3) Conduction was of low importance in the total heat balance (Figure 2). Therefore, assuming the ground temperature to be a linear function of soil depth or even neglecting the conductive heat flux had minor impacts on accuracy (Table 2).
(4) The heat flux associated with rain was minimal (Figure 2) and could be neglected from the model with little loss of accuracy (Table 1).

Sensitivity Analysis. A sensitivity analysis was conducted in order to assess the relative significance of uncertainties in the input parameters, the results of which are presented in Figure 3. Uncertainty regarding the air emissivity (ε_a) generated the greatest variation in the overall temperature prediction. This variation is due to the predominance of the air radiation in the heat balance (more than 60% of the heat gain on average; Figure 2). Uncertainties from other physical parameters and meteorological data tested were of minor importance affecting accuracy by less than 0.5 °C. Because the uncertainty with the air emissivity can cause the temperature prediction to vary by more than 1 °C, it is unlikely that the accuracy of the new universal model could be further improved.

Temperature Prediction Accuracy and Algal Productivity. As discussed in the Introduction, evaluating the economical feasibility and sustainability of processes incorporating shallow algal ponds requires the ability to predict the productivity of these systems and their environmental impact. For example, Richmond et al.[25] showed heating a *Spirulina* culture in the morning increased productivity in a raceway pond by 20%. Furthermore, Zhang et al.[2] achieved a 50% increase in productivity by maintaining temperature in its optimal range (37−43 °C) during *Chlorella sorokiniana* outdoor cultivation instead of letting the temperature fluctuate with the ambient temperature (20−44 °C). As shown in Figure 4, on a daily time scale the prior models regularly exhibited inaccuracies of more than 5 °C. In particular, predicting solar irradiance theoretically[23] caused a significant overestimation of the solar heat flux and the pond temperature (Figure 4). Reversely, determining the evaporative and convective heat fluxes using the empirical expressions from Talati et al.[9] caused an overestimation of the heat losses and therefore an underestimation of pond temperature. Because it is generally accepted that the growth rate of microalgae doubles when temperature increases by 10 °C within a certain range (e.g., 10−30 °C for most commercial algal species[24]), this error of 5 °C could therefore translate into a productivity prediction inaccuracy of approximately 40%.

Temperature Prediction Accuracy and Rate of Water Evaporation. In addition to the need to predict temperature

Table 2. Accuracy of Temperature and Water Evaporation (Annual Average) Using Models Constructed by Replacing Selected Heat Fluxes with Alternative Expressions Used in Prior Models[a]

heat flux	expression (ref)	E_{day} (°C)	E_{night} (°C)	E_{inter} (°C)	evaporation (mm d^{-1})
solar radiation	theoretical (23)	1.8	1.7	1.5	2.6
evaporation/convection	(7)	2.8	2.9	2.9	1.3
	(8)	2.5	2.4	2.6	2.0
	(9)	2.6	2.6	2.5	2.8
	(10)	3.4	4.5	4.1	4.6
conduction	simple	1.7	1.7	1.5	2.3
	neglected	1.8	1.7	1.5	2.3
rain	neglected	1.4	1.3	1.2	2.2
new universal model	see Modeling Approach	1.3	1.3	1.2	2.2

[a] The alternative expressions for each heat flux are detailed in the Supporting Information (S8). E_{day} is the average error in the estimation of the afternoon peak temperature, E_{night} is the average error in the estimation of the pre-dawn minimum temperature and E_{inter} the average error in the temperature difference between the afternoon peak and predawn minimum (Supporting Information, S6).

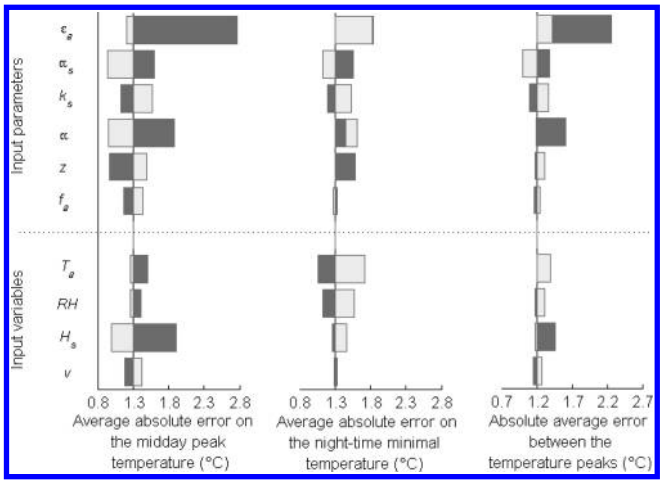

Figure 3. Sensitivity analysis on input parameters and input variables. The dark bars represent the level of accuracy for the maximum value of the parameter and the light bars the level of accuracy for the minimum value of the parameter [air emissivity (ε_a), 0.75−0.95; soil diffusivity (α_s), 10^{-7}−10^{-5} m^2 s^{-1}; soil conductivity (k_s), 0.2−4 W m^{-1} K^{-1}; power law exponent (α), 0.15−0.43; wind velocity height, 0.3−2 m; photosynthetic efficiency (f_a), 0−0.05; air temperature (T_a), ±1 °C; relative humidity (RH), ±10%; solar irradiance (H_s), ±10%; wind velocity (v), ±10%].

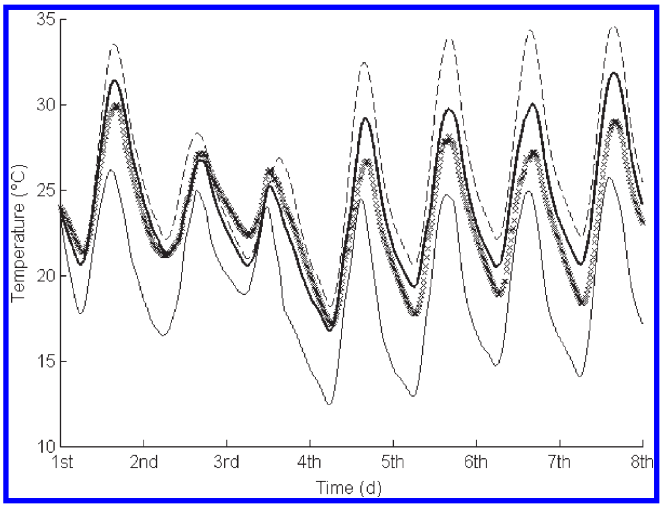

Figure 4. Predicted and measured temperature profiles in the high rate algal pond over the first week of January 2009 (crosses, experimental data; thick solid line, prediction by the new universal model; dashed line, prediction when a theoretical expression is used to determine the solar irradiance instead of on-site data;[23] thin solid line, prediction by the model when the expressions for convective and evaporative heat fluxes are taken from ref 9.

to estimate productivity, accurate temperature prediction is also required to estimate evaporative water loss. When using alternative heat flux expressions used in prior models, the predicted rate of evaporation from the high rate algal pond varied from 1.3 to 4.6 mm d^{-1} (Table 2). Under the temperate climatic conditions of Hamilton, New Zealand, the estimated annual average algal production was 220 kg (dry wt) (19 g m^{-2} d^{-1}) based on the amount of direct solar radiation reaching the pond (considering a photosynthetic efficiency of 2.5% and *Chlorella* biomass heat value of 20 kJ g^{-1} [26]). Thus, depending on the rate of water evaporation predicted by alternative heat flux expressions used in prior models, the estimate of the blue water footprint of the cultivation system varies from 70 to 240 L of water/kg of dry algal biomass. This variation of 300% is obviously problematic if an accurate estimation of the water evaporation losses is required at a high temporal resolution. Improved accuracy would be even more crucial for shallow algal ponds operated in semiarid or arid areas with limited freshwater resources.

In conclusion, the new universal model presented in this paper was validated with a high degree of accuracy with the average error at the afternoon peak and predawn minimum being just 1.3 °C, while the error between the afternoon peak and the predawn minimum was only 1.2 °C. This new universal model is valid for any opaque water body with a uniform temperature profile. Properly accounting for the evaporation appears to be the key to the new universal model and confirms that a theoretical approach is the most relevant to predict the rate of evaporation.[17] The inaccuracy on the temperature prediction introduced by the use of alternative heat flux expressions described in the literature could lead one to overestimate or underestimate algal productivity and the rate of water evaporation by approximately 40% and 300%, respectively.

■ ASSOCIATED CONTENT

Supporting Information. S1, schematic representation of the pond and heat fluxes considered in the heat balance; S2, significance of the solar radiation reflected on the water surface compared with the solar irradiance reaching the pond surface; S3, estimation of the air emissivity; S4, boundary condition of the heat equation in the soil layer under the pond; S5, data selection to determine the accuracy and month-by-month temperature profiles; S6, definition of the criteria for model accuracy; S7, prior temperature models published in the literature for ponds and similar systems; S8, alternative expressions from prior models for the solar heat flux, the evaporative and convective heat fluxes and the conductive heat flux. This material is available free of charge via the Internet at http://pubs.acs.org.

■ AUTHOR INFORMATION

Corresponding Author

*Telephone: +64 6 350 5841; fax: +64 6 350 5604; e-mail B.J.Guieysse@massey.ac.nz.

■ ACKNOWLEDGMENT

Q.B. is supported by a Massey University Doctoral Scholarship. We would like to acknowledge Dr. Marie-Laurence Giorgi (Ecole Centrale Paris, France) for very valuable discussions on thermal heat transfers. The high rate algae pond construction and operation were funded by New Zealand government funded research grant.

■ REFERENCES

(1) Raven, J. A.; Geider, R. J. Temperature and algal growth. *New Phytol.* **1988**, *110* (4), 441–461.

(2) Zhang, K.; Kurano, N.; Miyachi, S. Outdoor culture of a cyanobacterium with a vertical flat plate photobioreactor: Effects on productivity of the reactor orientation, distance setting between the plates, and culture temperature. *Appl. Microbiol. Biotechnol.* **1999**, *52*, 781–786.

(3) Torzillo, G.; Pushparaj, B.; Bocci, F.; Balloni, W.; Materassi, R.; Florenzano, G. Production of *Spirulina* biomass in closed photobioreactors. *Biomass* **1986**, *11*, 61–74.

(4) Vonshak, A.; Torzillo, G.; Masojidek, J.; Boussiba, S. Sub-optimal morning temperature induces photoinhibition in dense outdoor cultures of the alga *Monodus subterraneus* (Eustigmatophyta). *Plant Cell Environ.* **2001**, *24*, 1113–1118.

(5) Taine, J.; Iacona, E.; Petit, J. P. *Transferts Thermiques—Introduction aux Transferts d'Energie*, 4th ed; Dunod: Paris, 2008.

(6) Gerbens-Leenes, W.; Hoekstraa, A. Y.; van der Meerb, T. H. The water footprint of bioenergy. *Proc. Natl. Acad. Sci.U. S. A.* **2009**, *106* (25), 10219–10223.

(7) Losordo, T. M.; Piedrahita, R. H. Modelling temperature variation and thermal stratification in shallow aquaculture ponds. *Ecol. Modell.* **1991**, *54*, 189–226.

(8) Klemetson, S. L; Rogers, G. L. Aquaculture pond temperature modelling. *Aquac. Eng.* **1985**, *4*, 191–208.

(9) Talati, S. N.; Stenstrom, M. K. Aeration-basin heat loss. *J. Environ. Eng.* **1990**, *116* (1), 70–86.

(10) Ali, H. H. A. Passive cooling of water at night in uninsulated open tank in hot arid areas. *Energy Convers. Manag.* **2007**, *48*, 93–100.

(11) Park, J. B. K.; Craggs, R. J. Wastewater treatment and algal production in high rate algal ponds with carbon dioxide addition. *Wat. Sci. Technol.* **2010**, *61*, 633–639.

(12) New-Zealand National Institute of Water and Atmospheric Research Web site, http://www.niwa.co.nz/education-and-training/schools/resources/climate.

(13) Andersen, R. A., Ed. *Algal Culturing Techniques*; Elsevier Academic Press: Amsterdam, 2005.

(14) Hase, R.; Oiakawa, H.; Sasa, C.; Morita, M.; Watanabe, Y. Photosynthetic production of microalgal biomass in a raceway system under greenhouse conditions in Sendai City. *J. Biosci. Bioeng.* **2000**, *89* (2), 157–163.

(15) Howell, J. R; Siegel, R. *Thermal Radiation Heat Transfer*, 4th ed; Taylor & Francis: New York, 2004.

(16) Béchet, Q.; Shilton, A.; Fringer, O. B.; Muñoz, R.; Guieysse, B. Mechanistic modeling of broth temperature in outdoor photobioreactors. *Environ. Sci. Technol.* **2010**, *44*, 2197–2203.

(17) Sartori, E. A critical review on equations employed for the calculation of the evaporation rate from free water surfaces. *Sol. Energy* **2000**, *68* (1), 77–89.

(18) Tang, R.; Etzion, Y. Comparative studies of the water evaporation rate from a wetted surface and that from a free water surface. *Build. Environ.* **2004**, *39*, 77–86.

(19) Holman, J. P. *Heat Transfer*, 10th ed.; MacGraw Hill Higher Education: Boston, 2010.

(20) Gipe, P. *Wind Power—Renewable Energy for Home, Farm, and Business*; Chelsea Green Publishing Co.: White River Junction, VT, 2004.

(21) Miller, D. H., Ed. *Energy at the Surface of the Earth—An Introduction to the Energetics of Ecosystems*; Academic Press: New York, 1981.

(22) Culf, A. D.; Gash, J. H. C. Longwave radiation from clear skies in Niger: a comparison of observations with simple formulas. *J. Appl. Meteor.* **1993**, *32*, 539–547.

(23) Fritz, J. J.; Meredith, D. D.; Middleton, A. C. Non-steady state bulk temperature determination for stabilization ponds. *Water Res.* **1979**, *14*, 413–420.

(24) Davison, I. R. Environmental effects on algal photosynthesis: Temperature. *J. Phycol.* **1991**, *27*, 2–8.

(25) Richmond, A.; Lichtenberg, E.; Stahl, B.; Vonshak, A. Quantitative assessment of the major limitations on productivity of *Spirulina platensis* in open raceways. *J. Appl. Phycol.* **1990**, *2*, 195–206.

(26) Illman, A. M.; Scragg, A. H.; Shales, S. W. Increase in *Chlorella* strains calorific values when grown in low nitrogen medium. *Enzym. Microb. Technol.* **2000**, *27*, 631–635.